PREDICTION OF AEROSOL FORMATION FROM THE RELEASE OF PRESSUR-IZED, SUPERHEATED LIQUIDS TO THE ATMOSPHERE

D. W. Johnson and R. Diener
Quest Consultants Inc. and Exxon Research and Engineering Company

Water, CFC-11, chlorine, methylamine, and cyclohexane
have been released from superheated storage as part of a
research program directed by the American Institute of
Chemical Engineers Center for Chemical Process Safety
(CCPS). The objective of the research program is to further
the understanding of the post release process. This paper
presents the results of the testing and compares the results
to the CCPS liquid release model.

Key words: aerosol, release, model, liquid, superheated,
experimental

INTRODUCTION

The accidental release of pressurized liquids from containment to the atmo-
sphere can result in the formation of flashed vapor, liquid rain-out to the
ground, and fine liquid droplets entrained in any flashed vapor as an aerosol.
The degree of flashing that will occur depends only on the storage temperature
and the material's normal boiling point. However, the mass rate and properties
from such an accidental release, required to estimate downwind hazard zones,
also depend on how much if any aerosol is produced. There are numerous
papers in the literature dealing with estimating aerosol formation (e.g., Kaiser
and Walker, 1978 [1]), but none propose a validated first-principles predictive
model for aerosol formation versus liquid rain-out.

The American Institute of Chemical Engineers Center for Chemical Process
Safety (CCPS) recognized this need and initiated a multi-phase research effort
to develop a first-principles aerosol predictive model. This research effort also
included development of data to allow for the validation of this model. This
paper will briefly describe the predictive model, entitled RELEASE, which was
developed for the CCPS by Creare Inc. It will then describe in detail the data
generated for CCPS to allow for validation of RELEASE, discuss how well the
model performs against the data, and suggest areas for future research.

THE RELEASE MODEL, AN OVERVIEW

A complete description of the RELEASE model is provided by Iannello, Diener,
et al. [2] The following briefly summarizes the basis for the model.

Figure 1 indicates the five major regions of an accidental release from containment. The source region or model calculates the mass outflow rate to the atmosphere. In the expansion region, the high momentum jet from the release opening depressures to atmospheric pressure. During this depressurization, some of the liquid flashes to vapor and some of the liquid can be atomized to fine droplets by a process called flash atomization break-up. In the entrainment region, ambient air is entrained into the jet. Depending on the release conditions, this can result in cooling or heating of the released jet. Any cooling that does occur could also result in the condensation of moisture from the ambient air. In the pool region, liquid droplets that are too large to be entrained with the vapor rain-out onto the ground, collect and evaporate. In the vapor cloud region, vapor and aerosol from the entrainment region as well as any vapor from the liquid pool region are dispersed into the atmosphere. The RELEASE model includes algorithms for the source, expansion, rain-out, and entrainment regions.

RELEASE calculates the mass outflow rate from a circular opening assuming either all-liquid flow, equilibrium two-phase choked flow, or non-equilibrium flow. The flow calculation algorithm used is a function of the storage pressure, the material's vapor pressure at storage temperature, and the discharge length from the containment vessel to the opening.

In the expansion model, one-dimensional energy and momentum balances are performed to calculate the quality and velocity of the material entering the entrainment region. A radial momentum balance is also performed to calculate the rate of expansion. Liquid droplet size from the entrainment region is estimated based on Weber number criteria for both non-flashing flow (air-droplet shear responsible for drop-break-up) and flashing flow (flash atomization responsible for droplet break-up).

The rain-out model assumes that rain-out is determined by the trajectories of droplets at the start of the entrainment region. A log-normal distribution is applied to the single droplet size calculated in the expansion region. All droplets with an inclination from horizontal greater than the jet spreading are assumed to rain-out. Droplet evaporation and coalescence are ignored.

Finally, the entrainment region calculates the complete condition of the jet as a function of axial distance. This includes droplet evaporation and condensation of moisture from the atmosphere. Air entrainment versus distance is estimated using the Ricou-Spalding correlation. No additional rain-out is assumed to occur in the entrainment region.

RELEASE utilizes the DIPPR data base for physical properties with a built-in library of eight materials. The program can only be used for single components. The user can readily add properties to the program.

EXPERIMENTAL EQUIPMENT

The experimental program was conducted in the summer of 1989 at Norman, Oklahoma, and at the U.S. Department of Energy (DOE) Liquefied Gaseous Fuels Spill Test Facility (LGFSTF) at Mercury, Nevada, during August and

September of 1990. Both test programs used similar equipment consisting of a liquid release tank and release piping, a method to measure liquid release rates, a liquid capture system, pressure and temperature control systems, and miscellaneous instrumentation.

Three release tanks were used. A 1.5 cubic meter water tank, a 0.3 cubic meter CFC-11 tank, and a 1.3 cubic meter chlorine, methylamine, and cyclohexane release tank. Each release tank was insulated with a minimum of 3.8 cm of fiberglass insulation. Figure 2 illustrates the general construction features of the release tanks. All tanks were constructed of mild steel, and all fittings made from either schedule 80 threaded pipe or 300 # flanges. The liquid release piping was directly connected to the release tank via a short flanged connection and kept as short as possible to minimize pressure drop in the line during the release. A remotely operated pneumatic valve controlled the liquid movement to the release orifice. Connections were provided for nitrogen pressurization, vapor venting, as well as liquid fill and drain piping. These activities could all be controlled remotely using pneumatically operated valves.

Liquid release rates for the water and CFC-11 tests were measured using a calibrated differential pressure transducer to indicate the rate of level change in the release tank. Chlorine, methylamine, and cyclohexane release rates were measured directly by suspending the release tank on load cells. Both methods of measurement performed adequately during each testing program.

Three liquid capture systems were used. The capture system used for the water and CFC-11 tests consisted of a sloped catch basin approximately 5 m by 15 m. The liquid collecting and running from this capture system was delivered at 3 m increments to collection pans. Figure 3 shows this capture system. Chlorine and methylamine drops were captured in liquid filled systems consisting of 5 pans each 3 m by 6 m and filled with a dilute sodium hydroxide solution (chlorine) or a dilute sulfuric acid solution (methylamine). Figure 4 illustrates this system. Each liquid filled pan was equipped with a 68 m³/hr circulation pump to provide one pit circulation every 5 minutes. Cyclohexane was captured in the same pans, but without a liquid fill. Each pan was raised 0.15 m on one side creating a slope to a drain. The liquid reaching each drain was directed to a weighing vessel suspended from a load cell.

A nitrogen pressurization system was provided to each tank. This system consisted of a release tank pressure transducer, pressure controller, and pressure control valve. High pressure nitrogen from either a K-bottle manifold or tube trailer was regulated by a pressure regulator and piped to the pressure control valve.

Liquid storage temperature for above ambient temperature boiling liquids (water, CFC-11, and cyclohexane) was controlled using electric immersion heaters. The liquid temperature for chlorine and methylamine was maintained by auto-refrigeration of the liquid. The liquid temperature controller activated a vapor vent valve cooling the liquid by evaporation. The natural convective movement set up by either the immersion heaters or the vapor venting provided adequate liquid circulation to prevent temperature stratification.

Additional test instrumentation consisted of: 1) pressure and temperature transducer mounted near the release orifice, 2) temperature transducers mounted at several levels in the release tank, 3) meteorological instruments, and 4) a downstream temperature array (Nevada tests only).

EXPERIMENTAL RESULTS

Experimental data relating the amount of released liquid reaching the collection system as a function of liquid storage conditions has been obtained for 5 chemicals: 1) water, 2) CFC-11, 3) chlorine, 4) methylamine, and 5) cyclohexane. The five chemicals represent a 134°C range in boiling points, a liquid density range from 695 to 1558 kg/m³, and a range of surface tensions from 19 to 59 dynes/cm. The results will be presented in the chronological order that they were obtained. The ambient atmospheric pressure for the water and CFC-11 tests was 96.6 kPa and for the chlorine, methylamine, and cyclohexane tests was 90.3 kPa.

Water

The experimental results for the water tests are presented in Table 1 and graphically depicted in Figure 5. The tests covered a wide range of test conditions including orifice temperatures from 105 to 215°C, orifice pressures from 185 to 2140 kPa, and orifice diameters of 3.2, 6.4, and 12.7 mm. The average temperature of water reaching the collection system was 30.1 ± 4.2°C. As Figure 5 shows, the amount of water reaching the collection system was (within the experimental accuracy of the tests) a linear function of the liquid superheat (boiling point at ambient conditions was approximately 98.8°C). This was a somewhat unsuspected result since the RELEASE model predicts a curve having the shape shown in Figure 6. Visual observations of the downstream water release showed that considerable water was leaving the stream (within 1.2 m of the release point) as large drops with little horizontal velocity. This indicated that condensation and/or coalescence was occurring in the stream. These effects could easily mask the aerosol production process as developed in the RELEASE model (Iannello, Diener, et al. [2]). Visual observations of the release stream and the water capture temperatures showed that the initial shattering of the liquid stream occurred between 28-39°C of water superheat (126.8 to 137.8°C); while the complete shatter of the liquid occurred at about 45°C of superheat (143.8° C). These two occurrences were apparently masked by the coalescence and condensation occurring in the released stream.

Orifice sizes of 3.2, 6.4, and 12.7 mm were used during the water series. No orifice diameter effects were observed in the data for this range of orifice sizes.

CFC-11

CFC-11 experimental results are presented in Table 2 and shown in Figure 7. Orifice temperatures between 16 and 82°C (superheats of 0 to 59°C) and orifice pressures between 164 and 554 kPa were used in this series of tests. The average liquid capture temperature was -14 ± 6°C. Actual stream temperatures would be somewhat lower due to warming of the liquid by contact with the capture surface.

TABLE 1 – Summary of Water Release Tests

Orifice Diameter (mm)	Release Temp (C)	Liquid Superheat (C)	Isenth Flash (%)	Liquid Capture (%)	Release Press (kPa)	Release Over P (kPa)	Release Rate (kg/s)	Ambient Temp (C)	Wind Speed (m/s)
3.2	114.5	16.1	3.0	97.0	184.5	15.2	0.07	32.2	4.9
6.4	125.5	26.7	5.0	86.0	253.1	13.1	0.354	22.5	4.1
3.2	125.8	27.2	5.1	85.0	253.2	12.4	0.099	35.0	4.6
6.4	137.0	38.3	7.2	81.7	346.8	11.7	0.420	26.9	3.6
3.2	137.0	38.3	7.2	77.0	347.1	13.1	0.115	33.3	5.9
6.4	147.8	49.4	9.3	77.0	460.4	7.6	0.488	27.7	4.1
12.7	159.9	61.1	11.6	72.0	631.1	12.4	2.408	30.0	2.6
6.4	160.0	61.7	11.6	75.9	632.9	10.3	0.568	24.7	6.4
3.2	170.0	71.1	13.5	58.0	809.7	16.5	0.157	36.1	5.1
6.4	170.2	71.7	13.6	68.7	807.0	8.3	0.658	23.3	5.7
12.7	170.6	72.2	13.7	69.0	816.1	13.1	2.75	35.5	3.9
6.4	171.0	72.2	13.7	62.0	821.5	9.7	0.654	36.9	5.4
3.2	181.1	82.2	15.7	61.0	1047.2	15.2	0.184	24.1	6.2
6.4	181.2	82.8	15.7	64.0	1062.3	29.0	0.797	26.1	3.6
12.7	182.1	83.3	15.9	65.0	1062.0	12.4	3.111	36.6	5.7
6.4	192.5	93.9	18.0	59.0	1361.2	34.5	0.901	26.9	4.1
3.2	192.7	93.9	18.0	58.0	1352.7	20.7	0.213	28.3	5.1
6.4	203.2	104.4	20.0	54.0	1697.6	33.8	0.995	24.7	2.3
6.4	214.6	116.1	22.4	47.0	2109.4	20.0	1.144	30.0	4.1
3.2	215.0	116.1	22.4	46.0	2140.3	35.9	0.267	32.2	6.7

TABLE 2 – Summary of CFC-11 Release Tests

Orifice Diameter (mm)	Release Temp (C)	Liquid Superheat (C)	Isenth Flash (%)	Liquid Capture (%)	Release Press (kPa)	Release Over P (kPa)	Release Rate (kg/s)	Ambient Temp (C)	Wind Speed (m/s)
6.4	35.8	13.3	6.4	62.0	163.5	11.7	0.270	15.5	6.2
6.4	41.2	18.8	9.1	51.2	190.4	10.1	0.320	16.1	6.7
6.4	46.7	24.3	11.8	51.4	224.1	10.7	0.370	17.2	5.1
6.4	51.6	29.1	14.1	47.5	254.9	9.0	0.400	15.5	5.1
6.4	54.1	31.7	15.4	32.3	269.7	5.1	0.440	26.6	5.7
6.4	57.5	35.1	17.1	30.6	302.0	10.8	0.460	20.8	3.3
6.4	62.9	40.5	19.7	10.8	343.9	6.4	0.510	21.6	3.3
6.4	65.2	42.7	20.8	4.7	362.5	4.5	0.530	28.3	5.1
6.4	65.2	42.8	20.9	4.6	366.7	8.1	0.530	28.6	5.7
6.4	67.9	45.5	22.2	3.8	392.7	8.2	0.540	22.7	1.8
6.4	75.6	53.2	26.0	0.1	470.6	3.4	0.610	22.7	5.1
6.4	81.8	59.3	29.1	0.0	554.1	12.0	0.670	25.0	4.6

The start of CFC-11 liquid stream breakup occurred at approximately 46°C and complete breakup occurred at about 65°C. As Figure 7 shows, the highest capture measured was 62 percent. The apparent loss of liquid even from release streams with no superheat is felt to be due to the heat and mass transfer occurring between the stream and the air after the stream breaks into discrete drops. A preliminary heat and mass transfer analysis done on a typical unflashed CFC-11 release stream showed that at least 50 percent of the observed mass loss could be attributed to this mechanism. Observations of the release stream after it reached the capture surface showed that additional stream breakup occurred due to the impact. The rebounding smaller droplets would also lose weight via heat and mass transfer.

Chlorine

Table 3 presents the chlorine experimental results. Figure 8 shows the percent of chlorine released that reaches the capture liquid as a function of the liquid superheat. Liquid temperatures at the orifice ranged from -26.1 to 16.1°C (superheats from 10.5 to 52.7°C). Orifice pressures between 179 and 661 kPa were used giving release overpressure of 52 ± 7 kPa. The percent of released chlorine that was captured did not exceed 23 percent. As discussed in the preceding section, the heat and mass transfer occurring between the chlorine liquid drops and the air resulted in a significant loss of mass during the trajectory from the release orifice to the capture surface. Release stream temperatures averaged -67°C for the test series and ambient temperatures during the chlorine tests remained at approximately 30.2°C. The temperature of initial liquid stream shatter occurred at about -10°C corresponding to a liquid superheat temperature of 27°C and an isenthalpic flash of 8.6 percent.

Methylamine

Methylamine release tests were conducted at orifice conditions between -2.7 and 22.6°C and 173 and 381 kPa. Release overpressures were controlled at 55 ± 7 kPa. Figure 9 shows the methylamine liquid capture as a function of the liquid superheat at the orifice. Table 4 details the experimental conditions for the tests. Both 6.4 mm and 12.7 mm orifice diameters were used in the methylamine tests. Within the experimental uncertainty of the tests, no differences in the orifice results were apparent. The temperature of initial liquid stream shatter is estimated as 8°C. This temperature corresponds to a liquid superheat of 17°C and an isenthalpic flash of 6.6 percent. The release stream temperatures recorded during these tests averaged -46.4 ± 1.3°C. Maximum liquid capture was about 54 percent. As with the CFC-11 and chlorine tests, the effects of heat and mass transfer between the air and the release stream are thought to be responsible for this effect.

Cyclohexane

Table 5 and Figure 10 summarize the cyclohexane release data. Orifice release temperatures varied from 80.6 to 125.3°C resulting in liquid superheats between 3.4 and 48.1°C. Orifice overpressures averaged 73 ± 9 kPa. All cyclohexane tests used 6.4 mm orifice diameters. Release stream temperatures averaged 12 ±

TABLE 3 – Summary of Chlorine Release Tests

Orifice Diameter (mm)	Release Temp (C)	Liquid Superheat (C)	Isenth Flash (%)	Liquid Capture (%)	Release Press (kPa)	Release Over P (kPa)	Release Rate (kg/s)	Ambient Temp (C)	Wind Speed (m/s)
6.4	-26.1	10.5	3.4	22.5	178.9	36.9	0.382	31.2	5.8
6.4	-22.2	14.3	4.6	20.2	215.5	50.1	0.440	28.1	6.0
6.4	-21.6	14.9	4.8	17.3	225.9	56.3	0.443	30.7	4.9
6.4	-16.7	19.9	6.4	22.1	257.0	51.6	0.487	30.5	7.7
6.4	-15.1	21.5	6.9	18.1	258.6	40.7	0.485	31.4	
6.4	-11.3	25.2	8.0	22.5	303.3	53.1	0.552	27.6	6.0
6.4	-5.7	30.8	9.8	21.7	358.6	53.9	0.604	30.4	9.9
6.4	-0.7	35.8	11.4	16.0	420.8	60.2	0.645	29.8	7.2
6.4	0.2	36.8	11.7	9.4	433.9	61.6	0.652	31.2	4.9
6.4	4.8	41.4	13.1	9.7	482.3	50.7	0.704	31.7	6.1
6.4	10.5	47.1	14.9	4.0	567.2	52.8	0.758	30.4	7.5
6.4	10.6	47.1	14.9	5.6	558.9	43.9	0.742	32.7	7.1
6.4	16.1	52.7	16.7	0.8	661.1	53.7	0.834	30.2	5.2

TABLE 4 – MMA Test Results

Orifice Diameter (mm)	Release Temp (C)	Liquid Superheat (C)	Isenth Flash (%)	Liquid Capture (%)	Release Press (kPa)	Release Over P (kPa)	Release Rate (kg/s)	Ambient Temp (C)	Wind Speed (m/s)
6.4	-2.7	6.1	2.4	54.8	173.1	53.8	0.247	28.1	7.0
6.4	1.9	10.7	4.1	50.2	200.6	55.2	0.276	28.7	8.2
6.4	7.3	16.1	6.2	47.6	235.8	54.5	0.305	28.7	9.0
6.4	9.8	18.6	7.2	44.9	258.6	57.9	0.321	28.8	8.7
12.7	10.2	19.1	7.3	39.9	248.9	44.8	1.246	33.3	4.6
6.4	12.7	21.5	8.3	34.7	286.1	61.4	0.350	28.4	9.5
6.4	13.2	22.0	8.5	27.2	299.9	71.0	0.359	30.3	9.2
6.4	15.4	24.2	9.3	36.0	299.9	51.0	0.354	32.6	5.7
12.7	15.6	24.4	9.4	34.5	293.7	42.7	1.368	34.2	2.0
6.4	15.8	24.7	9.5	30.4	306.8	53.8	0.360	28.6	7.4
6.4	18.1	26.9	10.3	28.2	336.5	61.4	0.377	28.3	7.4
6.4	20.7	29.6	11.3	20.7	358.5	55.2	0.400	31.8	4.3
12.7	21.4	30.3	11.6	27.5	358.5	47.6	1.534	33.5	3.6
6.4	22.6	31.4	12.0	17.9	381.3	57.2	0.405	31.6	6.0

TABLE 5 – Summary of Cyclohexane Tests

Orifice Diameter (mm)	Release Temp (C)	Liquid Superheat (C)	Isenth Flash (%)	Liquid Capture (%)	Release Press (kPa)	Release Over P (kPa)	Release Rate (kg/s)	Ambient Temp (C)	Wind Speed (m/s)
6.4	80.6	3.4	2.0	51.9	182.9	82.9	0.260	35.3	5.2
6.4	86.8	9.6	5.7	52.4	209.1	89.1	0.283	36.1	3.2
6.4	92.1	14.9	8.8	51.2	217.4	78.1	0.300	35.7	3.1
6.4	97.8	20.6	12.3	42.3	239.5	76.7	0.315	35.6	4.2
6.4	102.9	25.8	15.5	38.4	256.0	69.2	0.331	35.9	2.9
6.4	108.9	31.8	19.3	45.3	282.9	65.8	0.357	35.7	4.5
6.4	114.3	37.1	22.8	28.6	309.9	62.3	0.375	36.0	3.1
6.4	119.7	42.5	26.3	18.4	354.7	72.7	0.406	36.9	3.1
6.4	125.1	47.9	29.9	10.5	383.7	63.8	0.414	37.0	4.0
6.4	125.3	48.1	30.0	10.3	391.9	70.6	0.428	34.9	2.2

2°C. The initial liquid stream shattering occurred at a superheat of 19°C, an orifice temperature of 96°C. This temperature corresponds to an isenthalpic flash of 11.4 percent. Cyclohexane capture at the boiling point is estimated to be 53 percent.

DISCUSSION OF RESULTS AND COMPARISON WITH RELEASE MODEL

The five experimental data sets provide some interesting similarities. Each of the data sets presents a similar relationship between the liquid capture and liquid superheat at the release orifice. In general, the curve can be represented as shown in Figure 11. An initial slow decline in the rate of liquid capture, points A to B, is followed by a more rapid decline, points B to C. The point at which the liquid capture versus superheat changes slope can be thought of as the point at which the liquid stream begins to break apart near the release point. Up to that temperature, the liquid stream looks and behaves like a coherent liquid. After this temperature is reached, the stream behaves as a collection of droplets. Table 6 summarizes the liquid to droplet transition information resulting from the test programs.

Liquid capture curves were computed using the RELEASE model for each of the five test chemicals. The results of these calculations are compared with the experimental data in Figures 12 through 16. Although the RELEASE model is not capable of accurately modeling the experimental data, the trend of the data (water excepted) is faithfully reproduced. The current RELEASE model does not contain the necessary submodels to account for droplet heat and mass transfer, droplet agglomeration, or condensation. Therefore, it should not be expected to accurately model the experimental data. The RELEASE model should model the overall data trends and the superheat temperature where the liquid stream begins to break apart.

TABLE 6

Material	Transition Superheat (°C)	Transition Flash (%)
Water	28-39	5.3-7.3
Cyclohexane	19	11.4
CFC-11	22	10.4
MMA	17	6.6
Chlorine	27	8.6

Looking more closely at the CFC-11 and monomethylamine data sets and predicted curves as shown in Figures 17 and 18, it is apparent that the predicted curve, when translated to a position over the experimental points, accurately models the trends of the data.

The RELEASE model exhibits the capability of predicting current experimental data. Additional work is required before the RELEASE model will be a useful analytical tool.

AREAS FOR FUTURE RESEARCH

Although the RELEASE model shows promise in qualitatively predicting the amount of aerosol formed during the release of superheated liquids, it is not currently capable of quantitatively predicting the experimentally observed aerosol behavior. With the exception of water, RELEASE tends to overpredict liquid capture and tends to overpredict the amount of superheat required to produce stream shattering. To reduce the degree of liquid capture overprediction, submodels are required to handle the heat and mass transfer between the liquid drops and the air, the possible coalescence of drops, and the potential for droplet condensation from super saturated vapor. Additionally, to adjust the liquid shatter transition point, the relationship between the RELEASE predictions and model parameters such as 1) Weber number criteria for drop breakup, 2) nucleation site density, and 3) the bubble growth rate factor (Iannello, Diener, et al. [2]) need to be studied to determine the most appropriate set of parameters to use.

The RELEASE model assumes a log-normal distribution of drop sizes around the average. This assumption is based primarily on the work of Brown and York [3] with water releases. There is no reason to question the validity of this assumption at this point. However, if RELEASE predictions do not agree with data after the above areas of research have been completed, this area may require further investigation. The determination of particle size distribution in an aerosol stream is not a simple task. Such measurements would require careful control of both the release stream and the ambient weather conditions. Small scale screening tests in a laboratory followed by larger scale tests in a wind tunnel would be one way of securing the necessary experimental data.

REFERENCES

1.   Kaiser, G. D. and B. C. Walker; *Releases of Anhydrous Ammonia from Pressurized Containers – The Importance of Denser-Than-Air Mixtures;* Atmospheric Environment, V12, 1978, 2289-2300.

2.   Iannello, V., P. H. Rothe, G. B. Wallis, R. Diener, and S. Schreuber; *Aerosol Research Program: Improved Source Term Definition for Modeling the Ambient Impact of Accidental Release of Hazardous Liquids,* 6th International Symposium on Loss Prevention and Safety Promotion in the Process Industries, June, 1989, Oslo, Norway.

3.   Brown, R. and J. L. York; *Sprays Formed by Flashing Liquid Jets,* AIChE Journal, 8(2), 149-153.
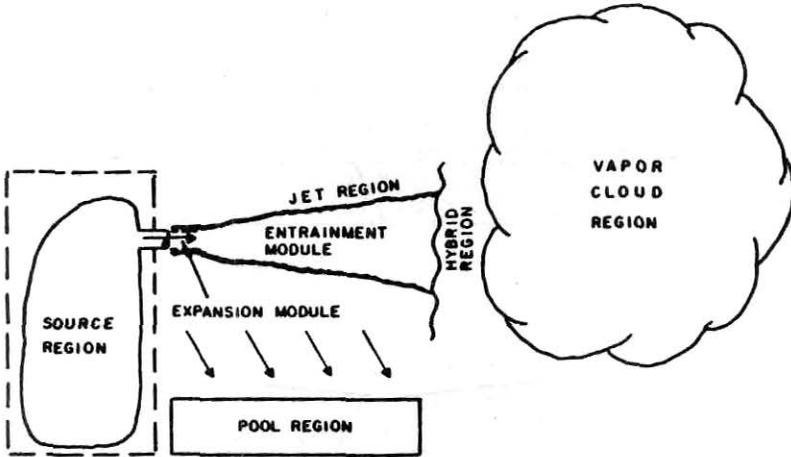
Figure 1 Regions of Interest
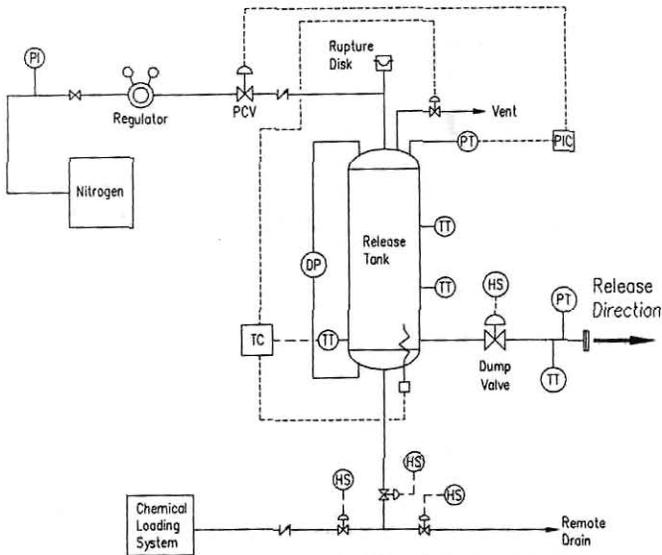
Figure 2 Release Tank
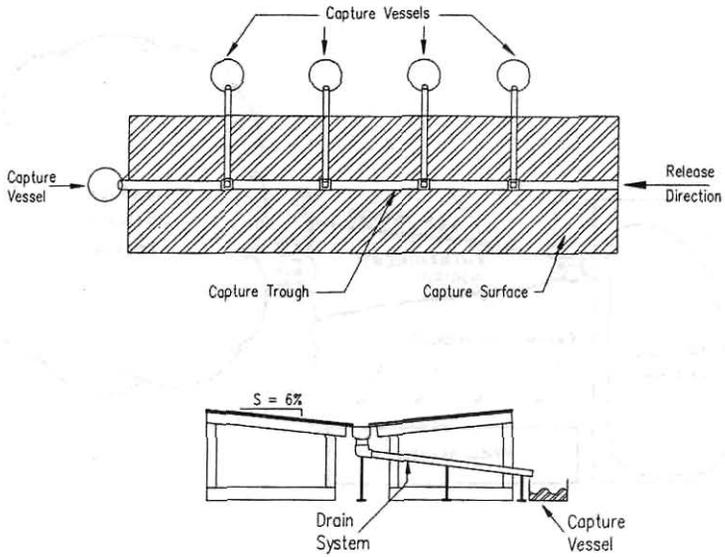
Figure 3 Water/CFC-11 Capture System
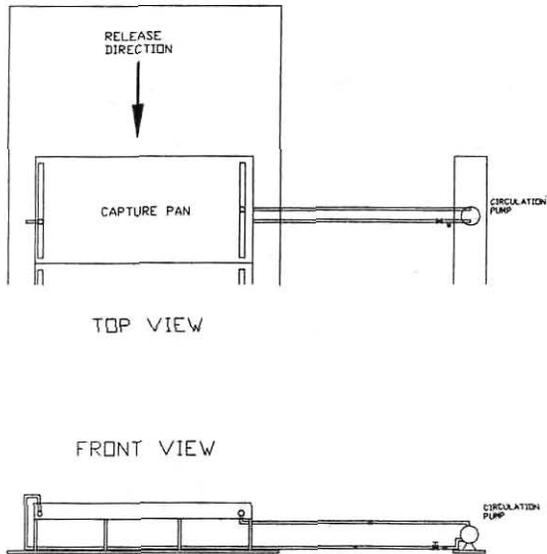
Figure 4 Chlorine/Methylamine/Cyclohexane Capture System
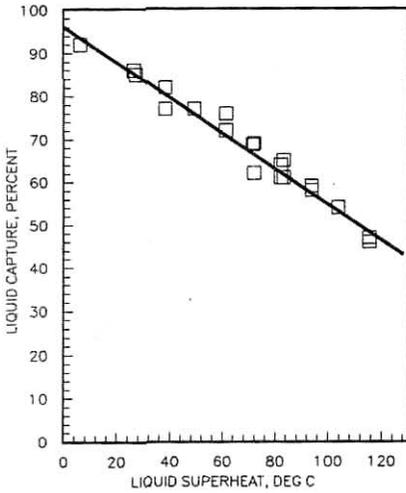
Capture is defined as the mass collected in the capture system divided by the total mass released from storage.

Figure 5 Water Experimental Data
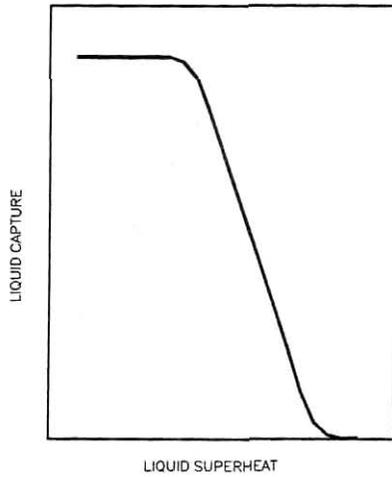
Capture is defined as the mass collected in the capture system divided by the total mass released from storage.

Figure 6 Expected Water Capture Curve
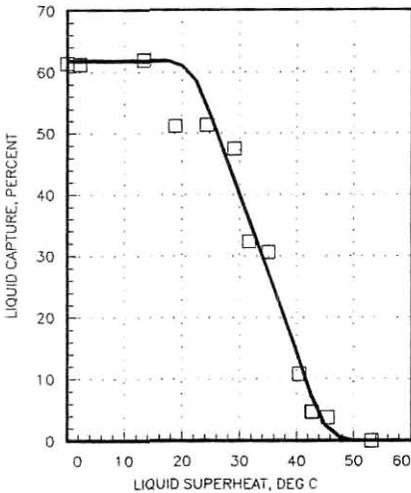
Capture is defined as the mass collected in the capture system divided by the total mass released from storage.

Figure 7 CFC-11 Experimental Data
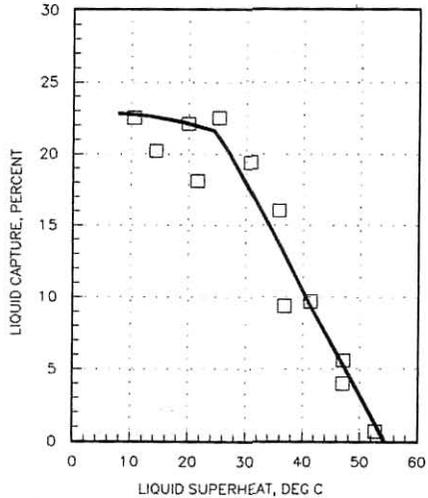
Capture is defined as the mass collected in the capture system divided by the total mass released from storage.

Figure 8 Chlorine Experimental Data
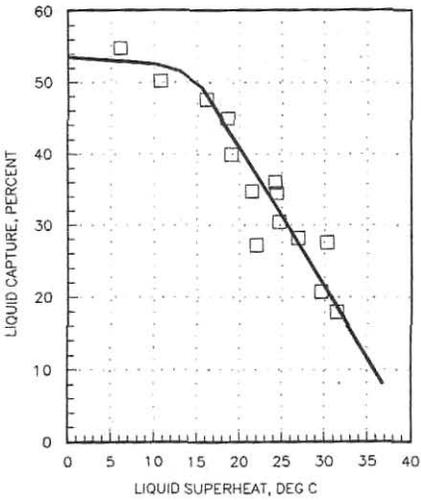
Capture is defined as the mass collected in the capture
system divided by the total mass released from storage.

Figure 9 Methylamine Experimental Data
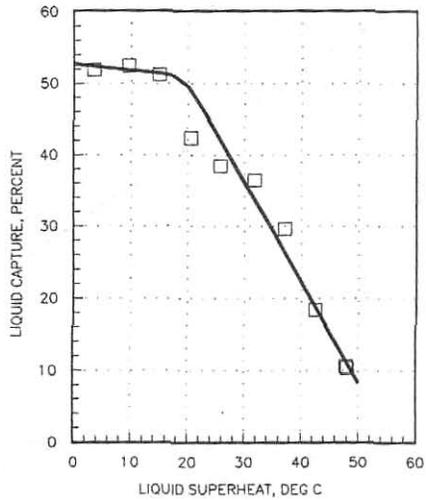
Figure 10 Cyclohexane Experimental Data
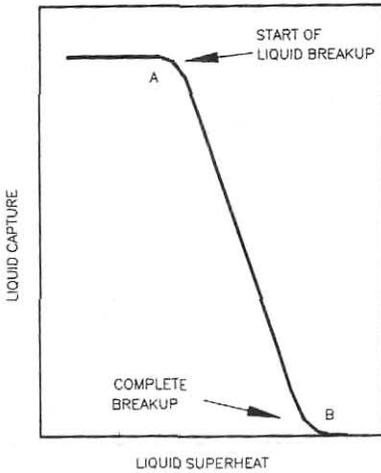
Capture is defined as the mass collected in the capture
system divided by the total mass released from storage.

Figure 11 Typical Capture Versus Superheat Curve
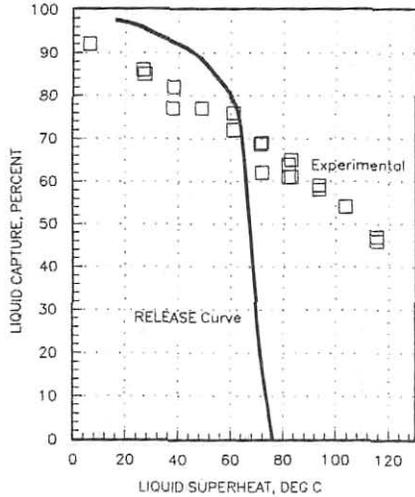
Capture is defined as the mass collected in the capture
system divided by the total mass released from storage.

Figure 12 RELEASE Comparison for Water
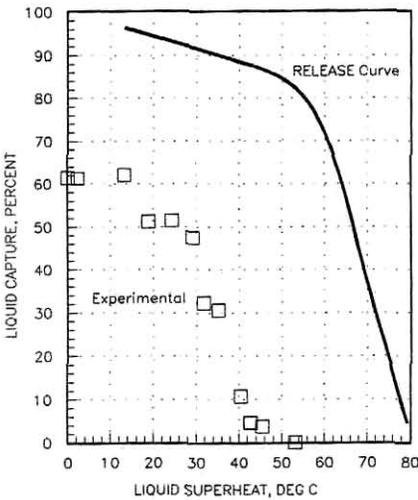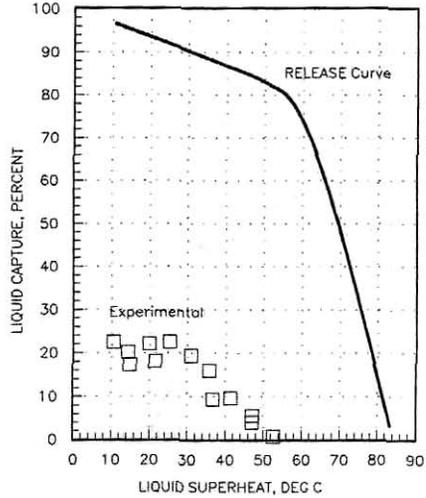
Capture is defined as the mass collected in the capture system divided by the total mass released from storage.

Figure 13 RELEASE Comparison for CFC-11

Capture is defined as the mass collected in the capture system divided by the total mass released from storage.

Figure 14 RELEASE Comparison for Chlorine
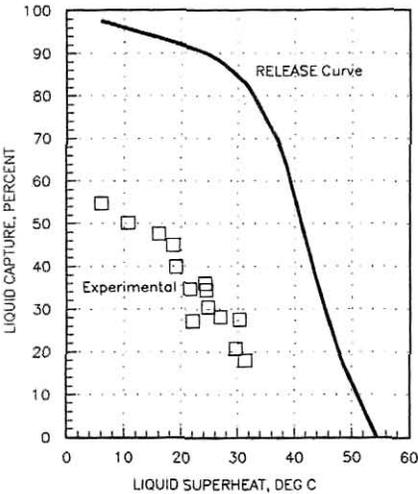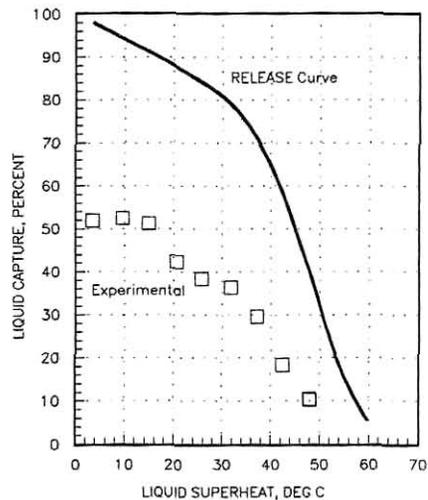
Capture is defined as the mass collected in the capture system divided by the total mass released from storage.

Figure 15 RELEASE Comparison for Methylamine

Capture is defined as the mass collected in the capture system divided by the total mass released from storage.

Figure 16 RELEASE Comparison for Cyclohexane
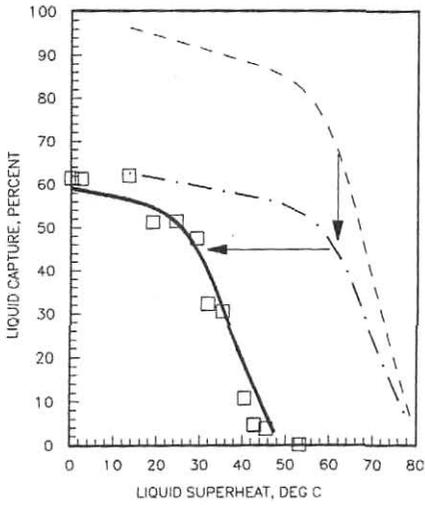
Capture is defined as the mass collected in the capture
system divided by the total mass released from storage.

Figure 17 Superposition of RELEASE Curve
on CFC-11 Data
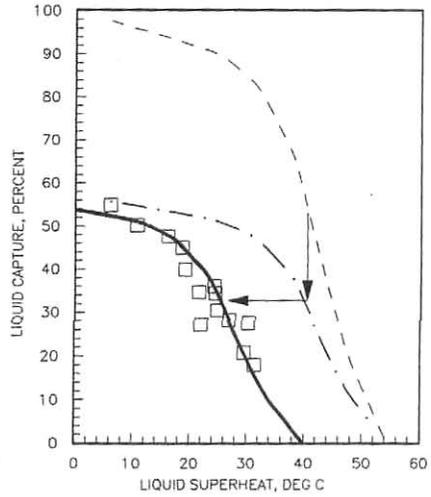
Capture is defined as the mass collected in the capture
system divided by the total mass released from storage.

Figure 18 Superposition of RELEASE Curve
on Methylamine Data